Supplementary

The complex resistomes of Paenibacillaceae reflect diverse antibiotic chemical ecologies

Andrew C. Pawlowski, Erin L. Westman, Kalinka Koteva, Nicholas Waglechner, and Gerard D. Wright

This file includes:

Supplementary Material and Methods

Supplementary Figures 1 – 10

Supplementary Tables 1 – 7

Additional supplementary information not included in this file:

Supplementary Dataset 1 - 2

Supplementary Materials and Methods

Antibiotics and reagents. All reagents were purchased from BioShop (Burlington, Ontario, Canada) unless otherwise specified. All antibiotics were purchased from Sigma-Aldrich (Oakville, Ontario, Canada), except for ampicillin and kanamycin (Bioshop) used for plasmid selection in *E. coli*. Organic solvents were purchased from Fisher Scientific (Ottawa, Ontario, Canada). Telithromycin was purified from the pharmaceutical formulation Ketek (400 mg, Sanofi-Aventis US). Two pills were crushed, dissolved in acetonitrile at 40˚C and large molecular weight polymers were removed by passing through an Amicon Ultra-15 10 kDa centrifugal filter unit and lyophilized.

Growth conditions and genomic DNA isolation. *Brevibacillus brevis* VM4 (ATCC 35690) was cultured on tryptic soy agar (TSA; BD biosciences; Mississauga, Ontario, Canada) for two days at 30˚C. The cell pellet from 3 mL culture of *B. brevis* VM4 cultured in Peptone Yeast extract (PY) media (1% (w/v) peptone, 0.5% yeast extract, 0.5% NaCl, 50 µg mL^{-1} $MgCl_2$, 30 µg mL^{-1} $MnCl_2$, pH 7.2) was used for genomic DNA isolation using the DNeasy Blood & Tissue Kit (QIAGEN). *E. coli* TOP10 (Invitrogen) was used for cloning experiments, *E. coli* BL21(DE3) was used for protein overexpression, and *E. coli* BW25113 Δ*bamB*Δ*tolC* (Cox et al., 2017) was used for susceptibility determination of *mphJ*. *E. coli* strains were cultured in LB-Lennox (BioShop) with either 100 µg mL^{-1} ampicillin or 50 µg mL^{-1} kanamycin for plasmid selection. *Paenibacillus* sp. LC231 was cultured on TSA for 2 days, and colonies with multiple growth phenotypes were used for inoculation (Pawlowski et al., 2016).

Antimicrobial susceptibility testing. Antibiotic susceptibility testing followed the Clinical and Laboratory Standards Institute guidelines (Clinical and Laboratory Standards Institute, 2012) for determining the minimal inhibitory concentration (MIC) in microtitre plates (Sarstedt;

Germany). For *B. brevis* VM4 and *E. coli*, 2-3 colonies were resuspended in saline and diluted 1:200 into Mueller-Hinton Broth (MHB, BD biosciences). MIC values for *B. brevis* VM4 were read after stationary incubation at 30˚C for 2 days, and MIC values for *E. coli* were read after 24 hours at 37˚C.

Cloning of resistance genes and susceptibility testing. Cloning is summarized in Supplementary Table 6, which includes details on expression vectors, restriction enzymes, and oligonucleotides. Phusion polymerase (ThermoFisher) was used to amplify genes from genomic DNA, digested with Fast Digest enzymes (ThermoFisher), and ligated into vectors using T4 DNA ligase (ThermoFisher). All pET vectors were transformed into *E. coli* BL21(DE3) for MIC experiments. pGDP4 (Cox et al., 2017) vectors were transformed into *E. coli* TOP10 for MIC experiments except for MphJ, which was transformed into *E. coli* BW25113 Δ*bamB*Δ*tolC*. RphC and RphD were synthesized as gBlocks (IDT) in two parts, codon optimized for *E. coli*. An internal engineered BamHI site was used to ligate both parts together, then ligated into pET28a using NdeI/XhoI restriction sites. Susceptibility testing was performed as described above.

Genome sequencing and prediction of resistance genotype. The *B. brevis* VM4 genome was sequenced using Roche 454 technology. Genomic DNA was sheared to 1.5 kb using a Covaris S220 ultrasonicator (Covaris), and used in library preparation according to the XL+ Rapid Library Preparation Method (454 Life Sciences/Roche). Emulsion PCR and sequencing were performing according to the manufacturer's instructions for the FLX+ instrument. MIRA version 3.4.9 was used for de novo assembly of the *B. brevis* VM4 genome. Resistance genotype was predicted using the Comprehensive Antibiotic Resistance Database (CARD; https://card.mcmaster.ca/) v3 (Jia et al., 2017).

Pan-Paenibacillaceae resistance genotype comparison. Orthologs of 15 experimentally validated resistance enzymes from *B. brevis* VM4 and *Paenibacillus* sp. LC231 were identified by querying all homologs curated in the CARD database against the nr protein database using BLASTp (ncbi-blast-2.2.31+), with the following conditions; -comp_based_stats turned off, txid186822[Organism] (Paenibacillaceae family) as an –entrez_query –evalue 1×10^{-75}, and –max_target_seqs 350. An ortholog was defined as having at least 50% identity with an alignment length of at least 90% of the query sequence length. Orthologs were identified in genome sequences by parsing the GenBank format feature table for accession numbers identified above. *vanA* vancomycin resistance clusters were identified by querying D-alanine-D-lactate ligases (*vanA* homologs) in the CARD database against Paenibacillaceae genomes as described above. A vancomycin resistance cluster was defined as having *vanRS* and *vanHAX*, which were identified using BLASTx against CARD. The *van* operon of *Brevibacillus* sp. SKDU10 (assembly ID: GCF_001645205.1) was found on the ends of two contigs; *vanHAX* was on one, and *vanRS* was on the other. Pair-wise sequence identity was computed with Clustal Omega percent identity matrix (Sievers et al., 2011). Genomic context was extracted from GenBank files. Genes from *B. brevis* VM4 were annotated using manual BLASTx searches on the web server and the transfer annotation function in Geneious v8.1.6.

Phylogenetic reconstruction of Paenibacillaceae rifampin phosphotransferases (Rph). Rph sequences identified in the pan-Paenibacillaceae resistance comparison were aligned with MAFFT using the L-INS-i method (Katoh and Standley, 2013). The alignment was then weighted using the transitive consistency score function of T-coffee (Chang et al., 2014). A maximum-likelihood tree was made with RAxML with the GAMMA model of rate

heterogeneity and JTT empirical base frequencies (PROTGAMMAAUTO flag) and using rapid bootstrap analysis on 100 replicates (Stamatakis, 2014).

Co-localization of resistance genes and mobile genetic elements. Genomic locations of each resistance gene were identified using efetch, and downloading the identical protein report (Maglott et al., 2007). The regions 2.5kb, 5kb, and 10kb upstream and downstream of each resistance gene were individually downloaded directly from GenBank using efetch. Mobile elements were identified in these regions by parsing GenBank CDS 'product' qualifiers for terms describing mobile genetic elements (Li et al., 2017, Hu et al., 2016, Forsberg et al., 2014); 'transposase', 'transposon', 'conjugative', 'integrase', 'integron', 'recombinase', 'conjugal', 'mobilization', 'recombination' and 'plasmid'. The terms 'integrase', 'recombinase', and 'transposase' were the most dominant. A resistance gene with nearby mobile genetic elements were identified as having one or more CDS with one of the terms described above. Plasmid localization of resistance genes was investigated by searching the 'source' feature of each GenBank file for 'plasmid_type' or 'plasmid', which is standard GenBank annotation for a plasmid (http://www.insdc.org/files/feature_table.html). Resistance genes with nearby mobile elements were then mapped onto the pan-Paenibacillaceae resistance genome comparison (Fig. 3). Mobile genetic elements near *van* operons were identified similarly, but the regions analyzed for mobile elements were upstream of *vanR* and downstream of the vancomycin resistance gene on the rightmost border of the cluster.

This approach is limited by the fact that most of the genome sequences in this study are assembled from short reads, and plasmids are therefore difficult to identify. Since only 42 of the 184 genomes were assembled into single chromosomes, two extra steps were taken to investigate whether resistance genes were on plasmids. The size of contigs that contain resistance genes

were extracted from GenBank files, and are summarized in Supplementary Figure 8. Resistance genes on contigs greater than 500 kb were assumed to not be mobile (Smillie et al., 2010). Contigs that contain resistance genes and were less than 500 kb were searched (megaBLAST) against all known RefSeq plasmids. Known bacterial RefSeq plasmids were downloaded from GenBank using the entrez query 'plasmid' (18,484 plasmids). None of the contigs were similar to known plasmids, and we did not find any evidence of horizontal transfer of resistance genes on plasmids.

Pan-*Brevibacillus* secondary metabolism comparison. AntiSMASH 3.0.5 with default settings and the –knownclusterblast flag was used to predict biosynthetic clusters from downloaded GenBank files (Weber et al., 2015). Biosynthetic clusters were grouped by sorting all sequences by length and using an all-against-all BLASTn with the following conditions; -task blastn, -max_hsps 10, and –evalue 1×10^{-25}. BLASTn results of homologous biosynthetic clusters can be split into multiple sub-alignments if small localized regions do not align well. These regions usually correspond to intergenic or other non-functional regions that are not essential to cluster function. Therefore, biosynthetic clusters were grouped together if the total length of sub-alignments (>70% sequence identity) was greater than 60% of the total sequence length. Groupings were validated manually by verifying genomic context and gene synteny in Geneious v8.1.6. Biosynthetic clusters linked to a known secondary metabolite were identified in the literature; gramicidin (Kessler et al., 2004), tyrocidine (Mootz and Marahiel, 1997), edeine (Westman et al., 2013), basiliskamides (Theodore et al., 2014), petrobactin (Lee et al., 2007). The presence of resistance genes in biosynthetic clusters were identified by searching the antiSMASH biosynthetic cluster GenBank files for protein accession numbers of resistance enzymes identified above.

Macrolide and kanamycin resistance gene expression experiments. For gene expression experiments, 2-3 colonies of *B. brevis* VM4 were resuspended in saline to an OD_{600} of 0.1, and 200 µL was used to inoculate 20 mL of MHB in a 50 mL Erlenmeyer flask. These cultures were incubated with shaking (250 rpm) at 30˚C for 16 hours, after which ¼ MIC erythromycin (0.063 µg mL^{-1}), tylosin (*B. brevis* VM4 0.125 µg mL^{-1}, *Paenibacillus* sp. LC231 4 µg mL^{-1}), or pikromycin (*B. brevis* VM4 2 µg mL^{-1}, *Paenibacillus* sp. LC231 32 µg mL^{-1}) were added and further incubated with shaking for 2 hours. An equal volume of DMSO was added to the no drug cultures. *mphI* expression experiments in *Paenibacillus* sp. LC231 were performed identically with ¼ MIC tylosin (4 µg mL^{-1}). After 2 hour incubation, 2 mL of culture were centrifuged at max speed and the cell pellets were stored at -80˚C until use. For RNA isolation, cell pellets were thawed, resuspended in 100 µL of 20 mg mL^{-1} lysozyme (25 mM tris pH 8.5, 1 mM EDTA) and incubated for 15 min at 37˚C. 20 µL of 20 mg mL^{-1} proteinase K was added to the cell mass and vortexed, and then incubated at 45˚C for an additional 5 min. Cells were lysed by the addition of 1 mL TRIzol (ThermoFisher) and repeatedly pipetting up and down. RNA was isolated by following the manufacturer's instruction for the TRIzol Reagent with the PureLink RNA mini kit protocol. RNA was eluted with 20 µL RNase-free water. The Maxima first-strand cDNA synthesis kit with dsDNase (ThermoFisher) was used for cDNA synthesis following the manufacturer's protocol with the following modifications; 5 µg of input RNA was DNase treated for 20 minutes at 37 ˚C and the reaction time at 50 ˚C was prolonged to 30 min. cDNA was diluted 5-fold before use in qPCR. Reactions contained 10 µL SYBR Select qPCR master mix, 8.2 µL 478 nM primers, 1.8 µL diluted cDNA. Each experiment was performed with biological triplicates. Gene expression was evaluated with the SYBR Select qPCR master mix (ThermoFisher) in a Bio-Rad C1000 real-time thermocycler with the following cycling

conditions; 50 ˚C for 2 minutes, 95 ˚C for 2 minutes, followed by 40 cycles of 95 ˚C for 30 s and 60 ˚C for 65 s, and one final extension for 1 minute. *gyrA* was used as in internal standard to normalize gene expression. qPCR negative controls were samples treated identically, but void of reverse transcriptase enzyme in the cDNA synthesis step. Oligonucleotide sequences are listed in Supplementary Table 7. Statistical analysis was performed using an unpaired Students t-test in GraphPad (https://www.graphpad.com/quickcalcs). Gene expression analysis of aminoglycoside modifying enzymes (*aac(6')-35* and *ant(4')-Ic*) was performed identically, but without the addition of any antibiotic.

***B. brevis* VM4 growth curves and *rph* expression**. *B. brevis* VM4 does not grow reproducibly in 96-well plates, and we therefore used Nephelo culture flasks (Pyrex) for growth curve experiments. 2-3 colonies of *B. brevis* VM4 were resuspended in saline to an OD_{600} of 0.1, and 200 µL was used to inoculate 20 mL of MHB in a 50 mL Erlenmeyer flask. These cultures were incubated with shaking (250 rpm) at 30˚C for 16 hours. 500 µL of this culture was used to inoculate 50 mL of MHB in a 250 mL Nephalo culture flask and incubated with shaking (250 rpm) at 30 ˚C. Cell growth was monitored by pouring culture into the attached sidearm and measuring OD_{600} (Spectronic 200, ThermoFisher). Rifampin (0.5x, 1x, or 2x MIC) was added at OD_{600} of 0.5 (6 hours). An equal volume of saline was added to the no drug control. All conditions were performed in duplicate. For *rph* expression analysis a similar experiment was performed on a culture challenged with 1x MIC rifampin. 2 mL of culture was removed prior to adding rifampin (pre-rifampin control), 2 hours post-rifampin challenge (lag phase), 5.33 hours post-rifampin (recovery phase), and 17 hours post-rifampin. RNA was isolated and cDNA synthesis were carried out as described above. *rphC* and *rphD* are 79% identical and we could not design primers unique to each gene. Degenerate primers (Supplementary Table 7) were used

to simultaneously amplify both *rphC* and *rphD* in the following reaction: 10 µL HF buffer, 1 µL 10 mM dNTP, 0.5 µL Phusion polymerase (ThermoFisher), 400 µM each primer, 2 µL of cDNA (first diluted 1:5), and water to 50 µL. Cycling conditions used were; 98 ˚C for 3 min, followed by 30 cycles of 98 ˚C for 20 s, 66 ˚C for 25 s, and 72 ˚C for 30 s, followed by a final extension of 1 min at 72 ˚C. Within the amplified region, *rphD* has a unique BamHI restriction site not found in *rphC* and this site was used to differentiate between *rphC* and *rphD* expression in the following reaction; 10 µL PCR product, 17 µL water, 2 µL of FastDigest Green buffer, and 1 µL FastDigest BamHI (ThermoFisher). The expected amplicon size was 396 bp for both *rphC* and *rphD* and digestion with BamHI would cleave *rphD* into two products (199 bp and 197 bp). Samples with and without BamHI digestion were run on a 2% agarose gel (FroggaBio). This experiment was performed with biological duplicates and a negative control where reverse transcriptase was not added to the cDNA synthesis reaction.

Monitoring rifampin degradation by *B. brevis* VM4. 2x MIC rifampin was added to 50 mL *B. brevis* VM4 cultures in mid-exponential phase similar to *rph* expression experiments above, and continued with shaking for an additional 36 hours. *B. brevis* VM4 cultured without rifampin, MHB with 2x MIC rifampin, and MHB were used as controls. 50 mL of acetonitrile was added to the culture flasks to lyse cells and extract hydrophobic compounds, including rifampin. Insoluble debris was removed by centrifuging at 10,000 × *g* for 20 minutes. The supernatant was lyophilized (Labconco) and resuspended in 1 mL water. The sample was centrifuged at 17,000 × *g* for 10 minutes resulting in three layers; sediment, liquid layer, and an upper solid lipid layer. The middle liquid layer was removed, lyophilized, and dissolved in 500 µL of 1:1 methanol:water. High resolution electrospray ionization mass spectra were acquired using Agilent 1290 UPLC separation module and qTOF G6550A mass detector in negative ion mode.

Liquid chromatography separation was carried out using Eclipse C18 (3.5 um, 2.1x100 mm) column (Agilent Technologies) and the following pump method: at 0 min 95% solvent A (0.1% v/v formic acid in water), from 1 to 7 min up to 97% solvent B (0.1% v/v of formic acid in acetonitrile), at a flow rate 0.5 ml/min. Rifampin eluted at 4.79 min and has $[M-H]^-$ m/z 821.39745.

To identify degradation products of rifampin phosphate, 5 µg mL^{-1} rifampin was added to a *B. brevis* VM4 culture in stationary phase. *B. brevis* VM4 was cultured for 16 hr in liquid MHB, at which point rifampin was added at 5 µg mL^{-1} and incubated with shaking (250 rpm) for 4 days at 30˚C. Samples were removed from the culture after 36 and 96 hours, and added to an equal volume of cold methanol and stored at -20˚C. Control samples that contained only MHB, MHB and 5 µg mL^{-1} rifampin, and only *B. brevis* VM4 were treated identically. Samples were centrifuged at 17,000 × *g* for 10 min to remove insoluble material. The presence of rifampin was monitored using HPLC. Samples were analyzed by injecting 50 µL onto an Agilent 1200 Series LC system (Agilent Technologies). The HPLC conditions are as follows: 95% water for 1 minute, linear gradient from 95% water to 100% acetonitrile from 1 min to 5 min, isocratic 100% acetonitrile to 5.5 min, linear gradient from 100% acetonitrile to 95% water to 6 min, then reequilibriation at 95% water until 12 min at a flow rate of 1 mL min^{-1} and using a C18 column (Waters Xterra RP 18, 5 µm, 4.6 x 150 mm).

Protein overexpression and purification. pET vectors were transformed into *E. coli* BL21(DE3) for overexpression, and 1 L cultures were incubated with shaking at 37 ˚C and 250 rpm until an OD_{600} of 0.5-0.6, chilled in an ice bath for 20 minutes, and induced with 1 mM IPTG for 16 hours at 17 ˚C. Cells were harvested by centrifuging at 10,000 × *g* for 20 minutes, washed with saline and resuspended in 20 mL buffer A (50 mM HEPES pH 7.5, 150 mM NaCl,

5% glycerol, 10 mM imidazole). Cells were lysed with a One-shot Cell Disruptor (Constant Systems Limited) at 20,000 psi and an additional 15 mL buffer A was added along with 5 mg bovine pancreas DNase (Sigma) and 2.5 mg of bovine pancreas RNase (Sigma). Cell debris and insoluble protein were removed by centrifugation at 48,000 × *g* for 45 min. Overexpressed proteins were purified with a 1 mL Ni^{2+}-nitrilotriacetic acid column (Qiagen) using a linear gradient of 95% buffer A to 100% buffer B (50 mM HEPES pH 7.5, 150 mM NaCl, 5% glycerol, 250 mM imidazole) over 20 column volumes. Fractions containing pure purified protein, as determined by SDS-PAGE, were pooled and desalted into 50 mM HEPES pH 7.5 using a PD-10 desalting column (GE Scientific). Pure enzyme stocks were stored at 4 ˚C.

Characterization of RphC and RphD reaction products. The regiospecific phosphorylation of rifampin by RphC and RphD was determined using mass spectrometry. Each 100 µL reaction consisted of 5 µg of total enzyme (either RphC, RphD, or 2.5 µg of each in a combined reaction), 0.5 mg/mL rifampin, and Rph Buffer (50 mM HEPES pH 7.5, 40 mM NH_4Cl, 5 mM $MgCl_2$ and 2 mM ATP). Reactions were incubated at room temperature for 16 hours, stopped with an equal volume of cold methanol, and stored at -20 ˚C. Samples were vortexed, and centrifuged at 17,000 × *g* for 10 min to sediment protein. 20 µL of each sample was injected onto an Agilent 1100 Series LC system and a QTRAP LC/MS/MS system (ABSciex). The HPLC conditions were as follows: isocratic 5% solvent B (0.05% formic acid in acetonitrile), 95% solvent A (0.05% formic acid in water) over 1 min, followed by a linear gradient to 97% B over 7 min at a flow rate of 1 mL/min and C18 column (Sunfire, 5 µm, 4.6 × 50 mm).

Steady-state kinetic characterization of resistance enzymes. Enzyme reactions were performed in duplicate, except for MphJ, which was performed in triplicate. All reactions were initiated with the addition of nucleotide (MphJ, ANT(4'), RphC, RphD) or acetyl-Coenzyme A

(acetyl-CoA). All enzyme reactions were performed in 96-well Nunc plates (Thermo Scientific) using Spectramax Plus384 (Molecular Devices) microtitre plate reader. GraphPad Prism was used for data analysis.

Steady-state kinetics for MphJ were measured using the PK/LDH (pyruvate kinase/lactate dehydrogenase)-coupled assay (Shakya and Wright, 2010). The phosphorylation of macrolide antibiotics was monitored by coupling the release of ADP/GDP with PK/LDH, and the oxidation of NADH was monitored at 340 nm using a SpectraMax plate reader in a 96-well format. Reaction mixtures contained 50 mM HEPES pH 7.5, 40 mM KCl, 10 mM $MgCl_2$, 0.2 mM NADH, 3.5 mM PEP, 4.8 U PK/LDH, 0.025 mg/mL MphJ. For macrolide dependence experiments, GTP or ATP were provided at 200 µM and macrolide concentration varied from 3.2 µM – 400 µM. For nucleotide dependence experiments, erythromycin was provided at 400 µM and nucleotide concentration varied from 7.8 µM – 4000 µM. Reactions were incubated at 37˚C for 5 min before initiating with nucleotide.

Steady-state kinetics for RphC and RphD was performed using the EnzChek Phosphate Assay Kit (Molecular Probes) in Rph Buffer with a final volume of 100 µL (Stogios et al., 2016, Spanogiannopoulos et al., 2014, Pawlowski et al., 2016). The rifampin K_m was determined by varying the concentration between 0.38 µM and 16 µM and maintaining ATP at 250 µM. The ATP Km was determined by holding the rifampin concentration at 8 µM and varying the ATP concentration between 3.13 µM and 250 µM.

Steady-state kinetics for AAC(6')-35 was measured by monitoring CoA liberation using DTDP in a 250 µL reaction at 25 °C containing 25 mM MES pH 6.0, and 1 mM EDTA (Wright and Ladak, 1997, Pawlowski et al., 2016). The K_m of acetyl-CoA was performed as follows: 20 µM kanamycin, 31.25 to 2,000 µM acetyl-CoA and 253 nM AAC(6′)-35. The K_m of kanamycin was

267 determined as follows: 500 μM acetyl-CoA, 1.25 to 250 μM kanamycin and 253 nM AAC(6′)-35.
268 Acetyl-CoA was not saturating when determining the K_m of kanamycin.

269 Steady-state kinetics for ANT(4')-Ic was measured using the EnzChek pyrophosphate assay
270 (Molecular Probes) in a 100 μL reaction at 25 ˚C containing 50 mM HEPES pH 7.5, 40 mM
271 KCl, 10 mM $MgCl_2$ (Cox et al., 2015). The K_m of ATP was determined as follows: 20 μM
272 kanamycin, 78.13 – 2500 μM ATP, and 245 nM ANT(4')-Ic. The K_m of kanamycin was
273 determined as follows: 2500 μM ATP, 0.23 – 30 μM kanamycin and 245 nM ANT(4')-Ic.

Supplementary Figures

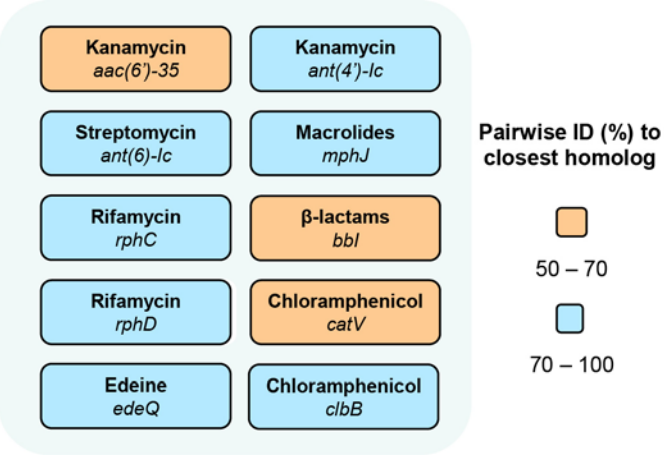

Supplementary Figure 1: The *B. brevis* VM4 resistome. Boxes represent each resistance determinant in this study, and the colour fill represents the percent identity to the closest experimentally validated homolog.

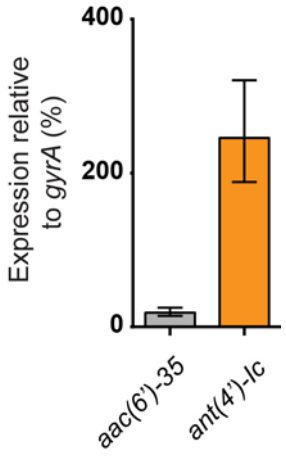

Supplementary Figure 2: *B. brevis* VM4 has two kanamycin resistance genes, an *aac(6')* and an *ant(4')*, that are expressed. Error bars represent one standard deviation.

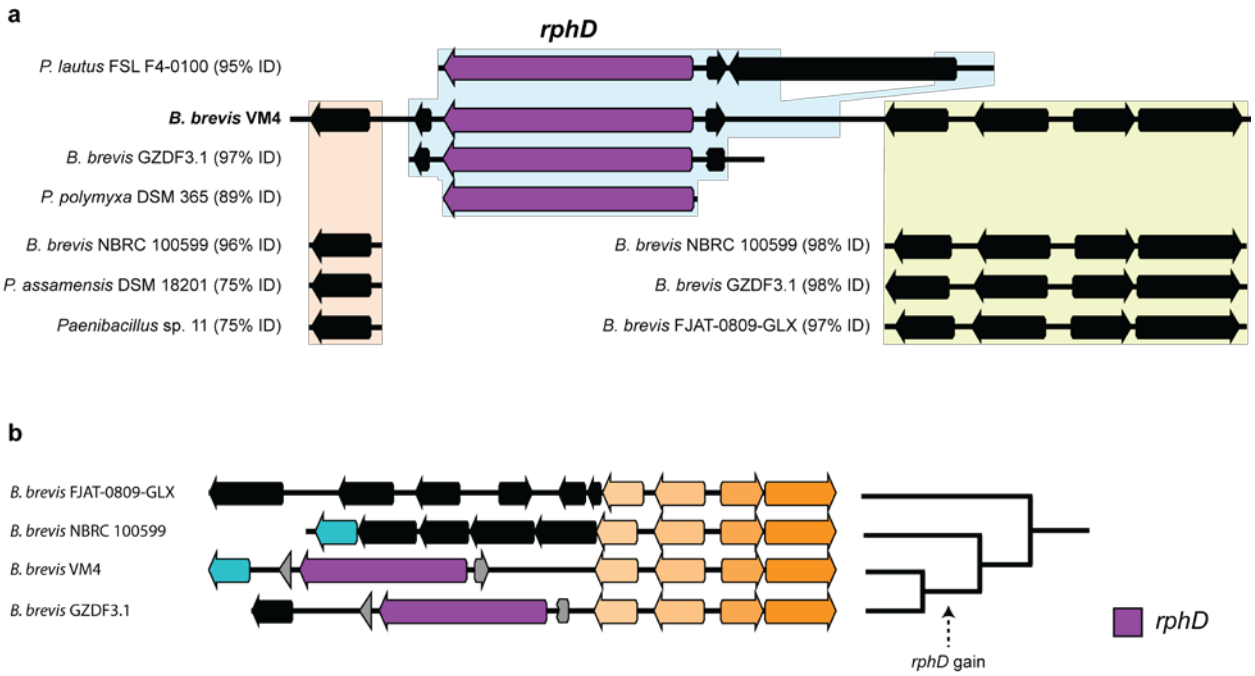

Supplementary Figure 3: *rphD* was horizontally transferred into a *B. brevis* VM4 ancestor. **a**, Genetic context of *rphD* and the top 3 BLASTn hits of the adjacent regions. The cluster of genes upstream from *rphD* is conserved among related *Brevibacillus*, and *rphD* and the region immediately upstream are conserved with *Paenibacillus* isolates and *B. brevis* GZDF3.1, which also has two *rph* pseudoparalogs. Percent identity of pair-wise DNA alignments with *B. brevis* VM4 are displayed. **b**, *rphD* was acquired by the *B. brevis* GZDF3.1 and *B. brevis* VM4 ancestor. Conserved gene orthologs are coloured. The GenBank coordinates are; *P. lautus* FSL F4-0100, NZ_MRTF01000005 551266 – 557081; *B. brevis* GZDF3.1, NZ_LVYG01000001 653739 – 657453 and 657467 – 661279; *P. polymyxa* DSM 365, NZ_JMIQ01000010 35305 – 37966; *Paenibacillus* sp. 11, NZ_FXAZ01000001 1295778 – 1296531; *P. assamensis* DSM 18201, NZ_AULU01000011 191516 – 192256; *B. brevis* NBRC 100599, NC_012491 3172554 - 3176406 and 3172543 – 3176420; *B. brevis* FJAT-0809-GLX NZ_AHKL01000056 32079 – 35873.

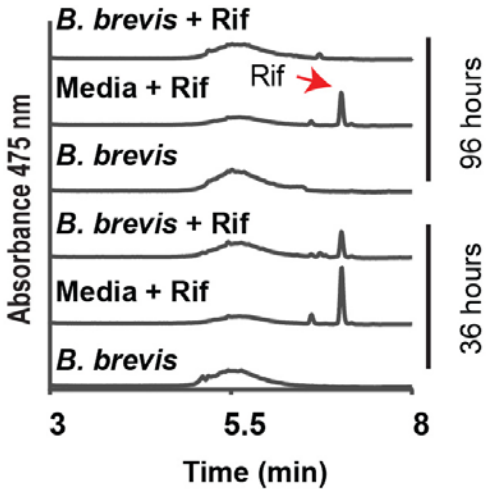

Supplementary Figure 4: HPLC analysis of *B. brevis* VM4 cultured with 5 µg mL^{-1} rifampin over 4 days.

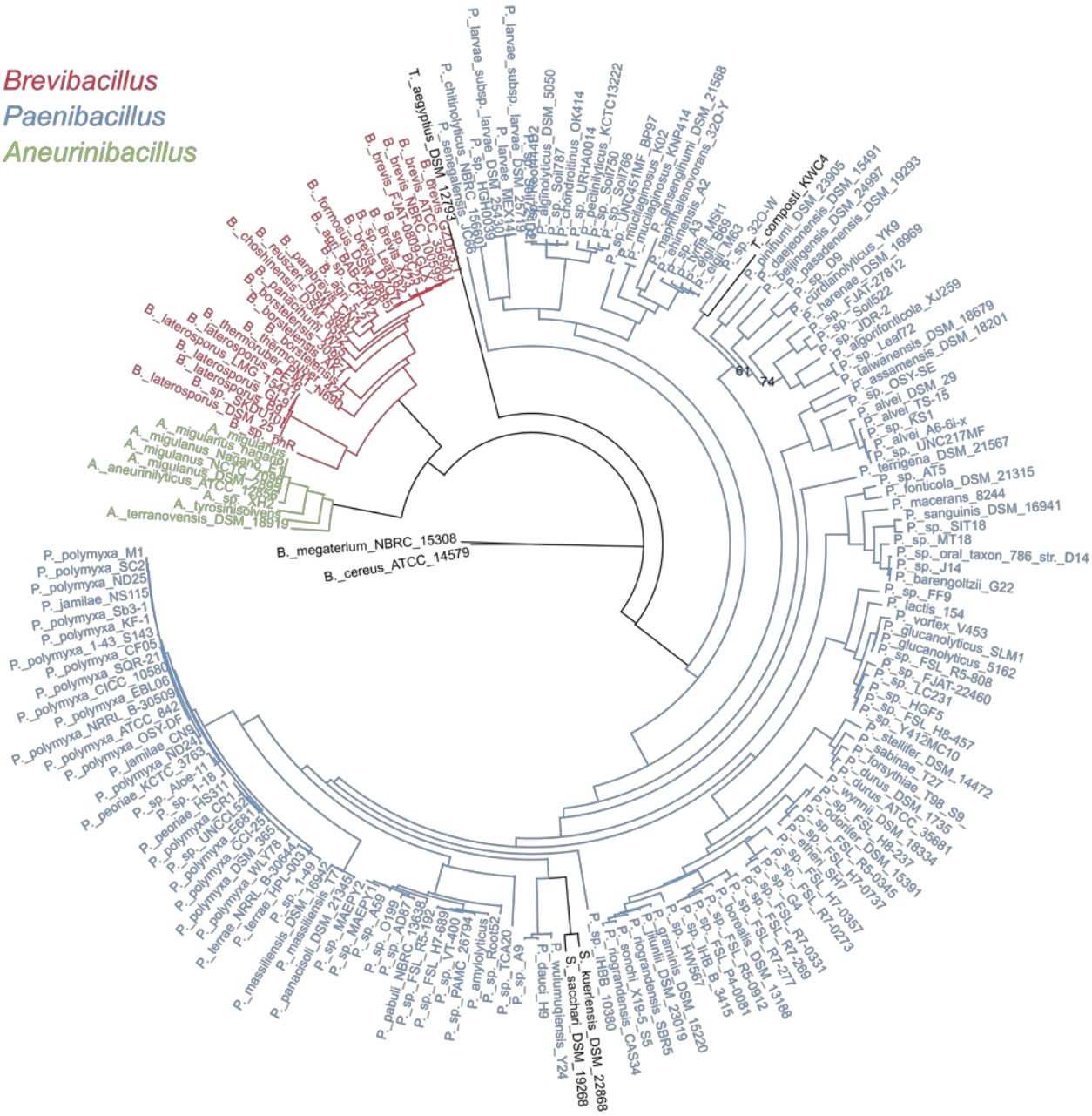

Supplementary Figure 5: Phylogenetic tree of 184 Paenibacillaceae isolates. Concatenated maximum-likelihood tree using 109 conserved genes, presented as a circular phylogram. The coloured segments highlight the three major genera in Paenibacillaceae; Paenibacillus (blue), Brevibacillus (red), and Aneurinibacillus (green). Bootstrap values below 90 are displayed at branch points, except for crowded branch points near the tips where bootstrap values are not displayed.

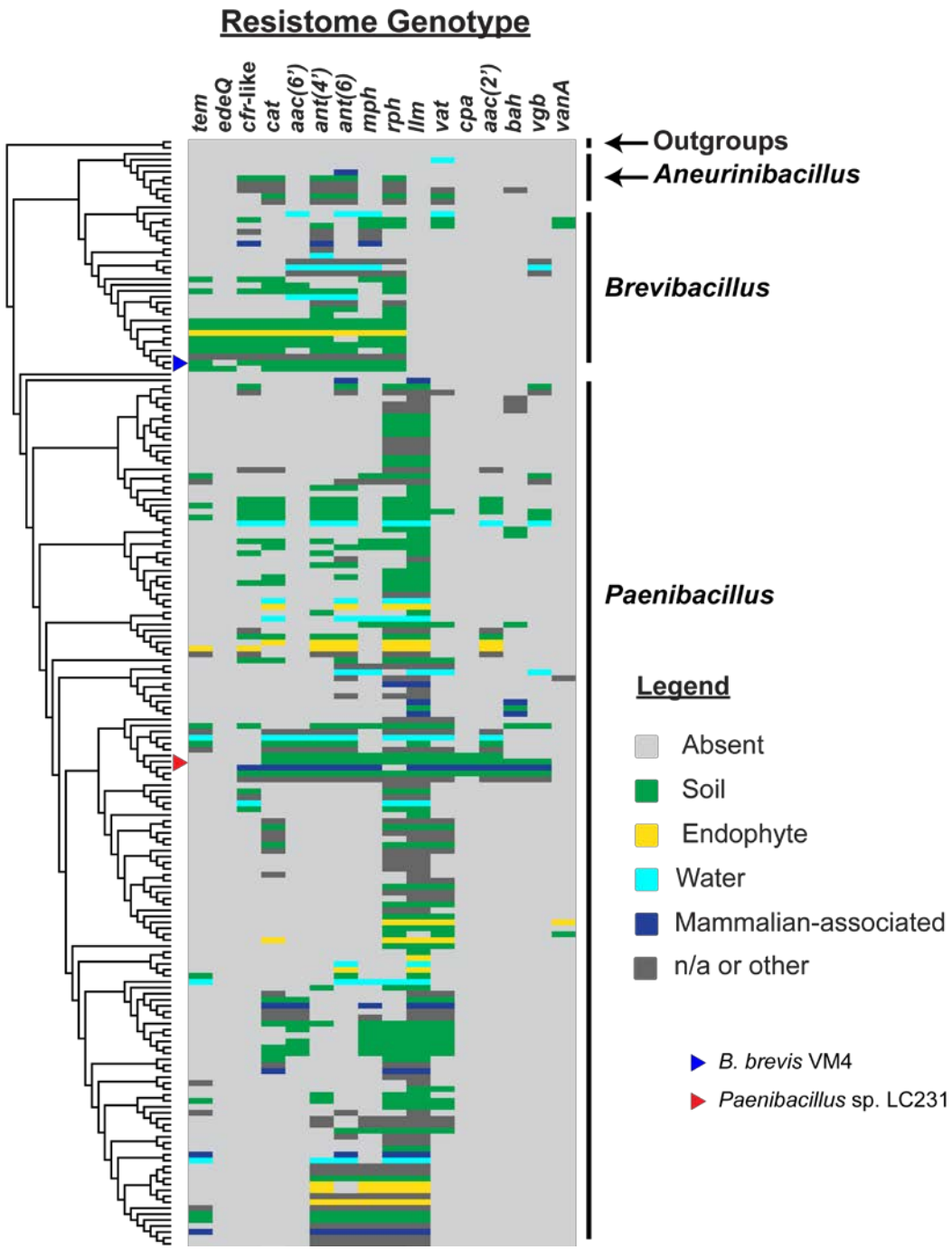

Supplementary Figure 6: Resistome comparisons highlighting the known habitat from which strains were isolated. The habitat was generalized from the 'isolation source' qualifier in GenBank files, if available, or from culture collection databases (e.g. DSM, ATCC) and mapped onto the Paenibacillaceae resistome comparison (Fig. 3). The original entries for isolation sources can be found in Supplemental Dataset 1. The tree is presented as a dendrogram.

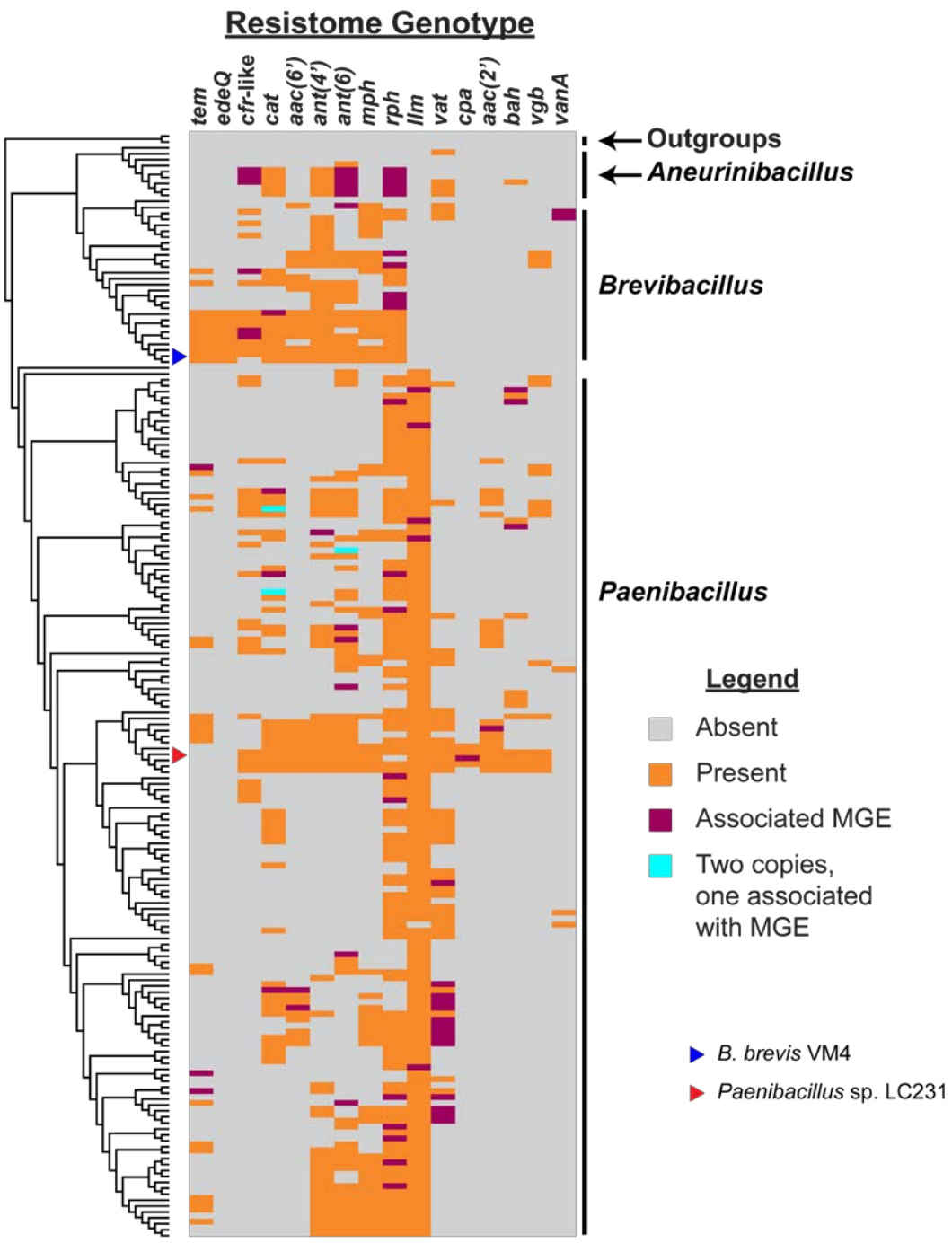

Supplementary Figure 7: Mobile element-associated resistance genes are randomly distributed across Paenibacillaceae. Resistance genes with nearby mobile genetic elements were mapped onto the Paenibacillaceae resistome comparison (Fig. 3) to visualize horizontal and vertical transfer of resistance genes. The tree is presented as a dendrogram.

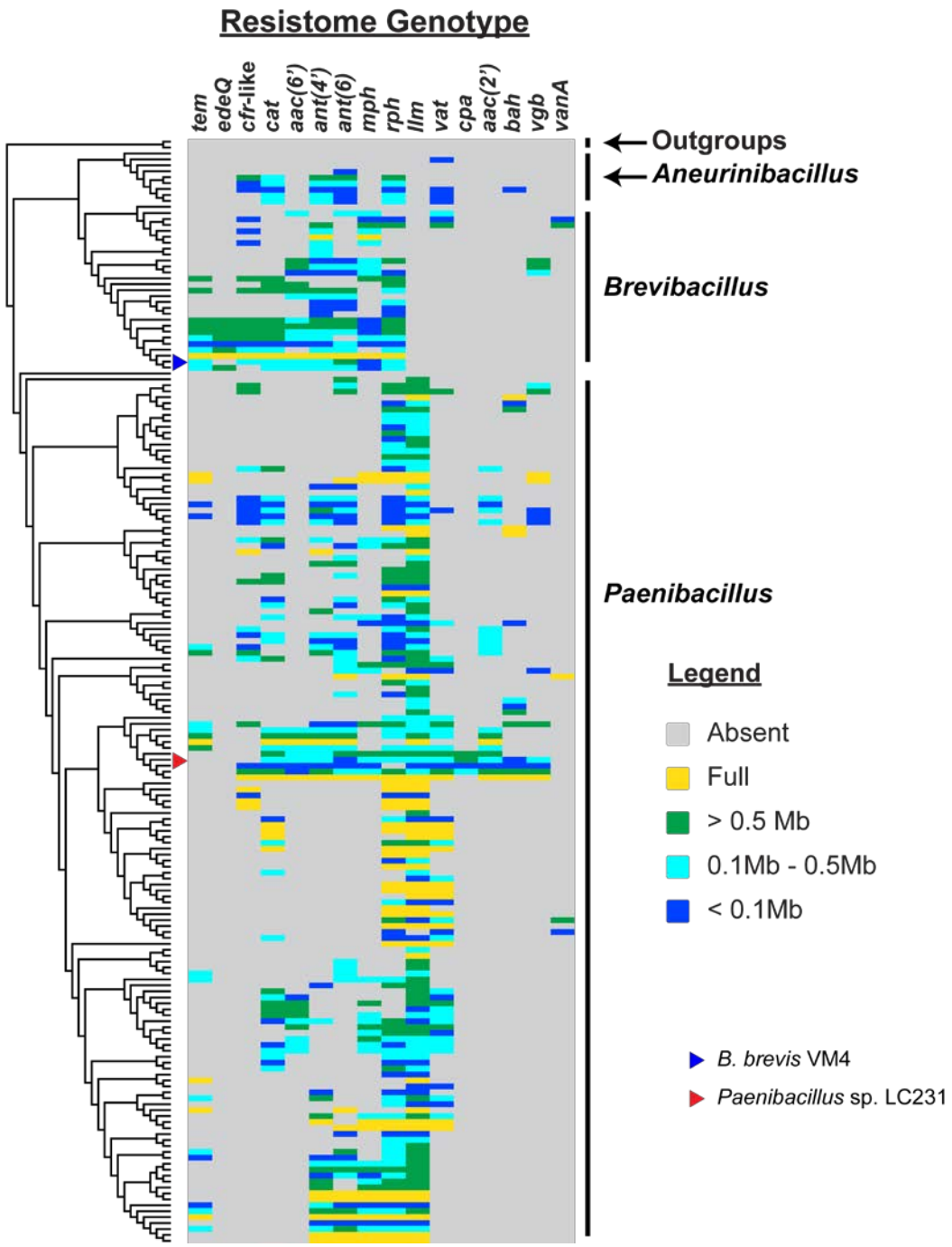

345

346 **Supplementary Figure 8**: Resistance genes are unlikely to be horizontally transferred on
347 plasmids. The sequence length of each contig with a resistance gene was identified from
348 corresponding GenBank files, and the resistome comparison was coloured to highlight resistance
349 genes on; complete chromosomes, contigs greater than 0.5 Mb, between 0.1 Mb and 0.5 Mb, and
350 less than 0.1 Mb. This was mapped onto the Paenibacillaceae resistome comparison (Fig. 3). The
351 tree is presented as a dendrogram.

352

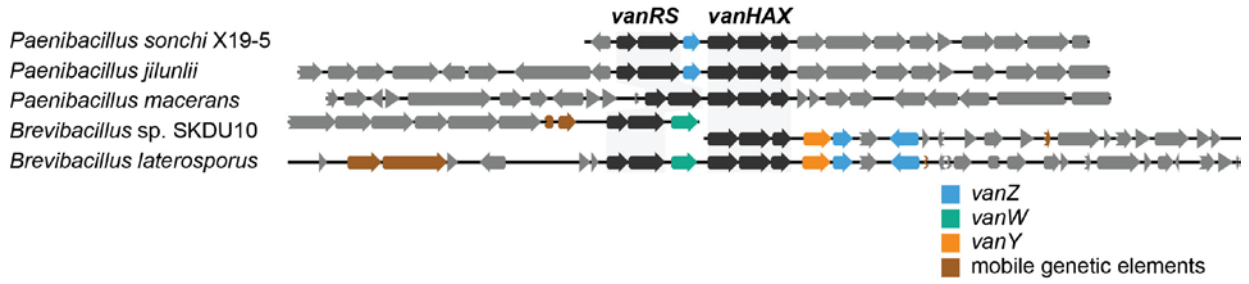

Supplementary Figure 9: Vancomycin operons identified in Paenibacillaceae isolates. Predicted vancomycin resistance genes and mobile genetic elements are coloured. The operons were found on the following accession numbers; *Paenibacillus sonchi* X19-5 (NZ_AJTY01000176), *Paenibacillus jilunlii* (NZ_LIPY01000123), *Paenibacillus macerans* (NZ_KN125580), *Brevibacillus* sp. SKDU10 *vanRS* (NZ_LSSO01000215) and *vanHAX* (NZ_LSSO01000140), and *Brevibacillus laterosporus* (NZ_JNFS01000003).

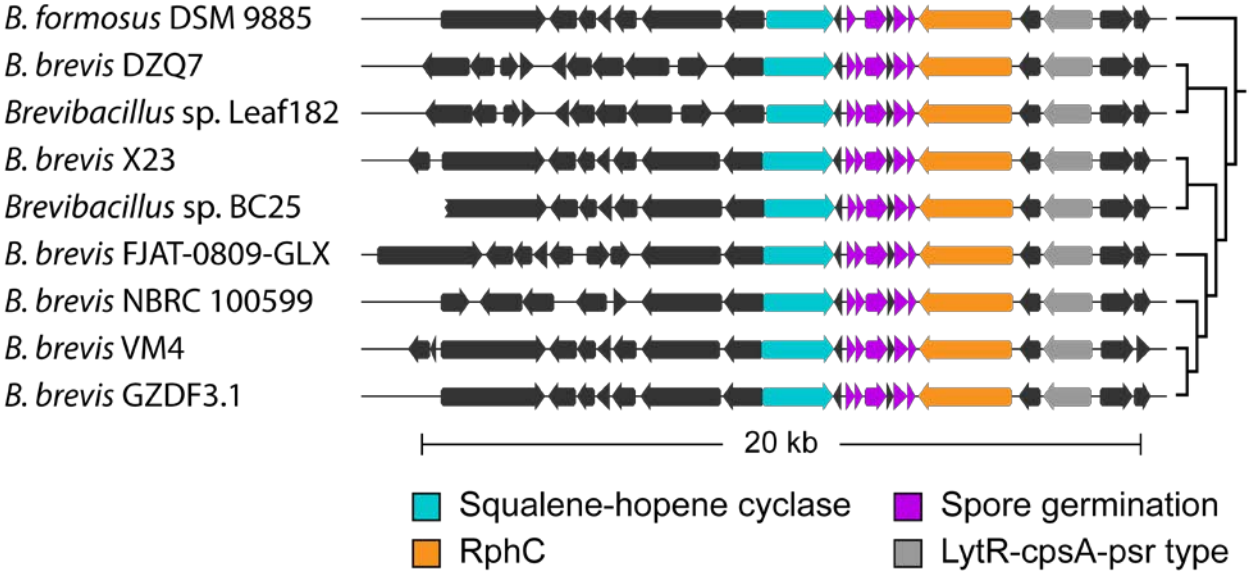

Supplementary Figure 10: RphC is clustered within a polycyclic terpenoid biosynthetic cluster. RphC is conserved within terpene group 89, which may produce a hopanoid-like secondary metabolite. The *B. brevis* VM4 species tree was extracted from the Paenibacillaceae tree and presented as a dendrogram. The predicted terpene cluster from *B. brevis* FJAT-0809-GLX was truncated from the left by 5 genes for presentation.

Supplementary Tables

Supplementary Table 1: Quantitative antibiogram of *Brevibacillus brevis* VM4 and CARD predicted resistance genotype.

Antibiotic	MIC (μg mL^{-1})	CARD prediction
Ampicillin	> 256	*bbI*
Piperacillin	128	*bbI*
Piperacillin/taxobactam	16	
Cefotaxime	< 0.5	
Meropenem	< 0.5	
Cephalexin	4	
Cefotaxime	< 0.5	
Lincomycin	> 256	*clbB*
Clindamycin	4	*clbB*
Synercid	8	*clbB*
Kanamycin	> 512	*aac(6')-35* and *ant(4')-Ic*
Neomycin	32	*aac(6')-35* and *ant(4')-Ic*
Gentamicin	4	*aac(6')-35* and *ant(4')-Ic*
Ribostamycin	>512	*aac(6')-35* and *ant(4')-Ic*
Isepamicin	256	*aac(6')-35* and *ant(4')-Ic*
Paromomycin	>512	*ant(4')-Ic*
Lividomycin	>256	*ant(4')-Ic*
Sisomicin	<0.5	*aac(6')*
Netilmicin	2	*aac(6')*
Streptomycin	32	*ant(6)-Ic*
Spectinomycin	> 256	
Fortimicin A	2	
Mupirocin	> 100	*ileRS*
Chloramphenicol	8	*catV*, *clbB*
Apramycin	4	
Fosfomycin	2	
Vancomycin	2	
Teicoplanin	< 0.5	
Tetracycline	2	
Tigecycline	< 0.5	
Minocycline	< 0.5	
Ciprofloxacin	< 0.5	
Erythromycin	0.25	*mphJ*
Telithromycin	< 0.5	*mphJ*
Tylosin	0.5	*mphJ*
Pikromycin	8	*mphJ*
Linezolid	< 0.5	*clbB*
Novobiocin	< 0.5	
Rifampin	0.063	*rphC* and r*phD*
Rifamycin SV	0.125	*rphC* and *rphD*

Supplementary Table 2: Pair-wise comparison of antibiotic resistance enzymes with their closest ortholog.

Resistance Enzyme	Closest Relative (% ID)	Host
ANT(4')-Ic	ANT(4')-Ia (71%)	*Bacillus clausii*
AAC(6')-35	AAC(6')-34 (54%)	*Paenibacillus* sp. LC231
ANT(6)-Ic	Aadk (72%)	*Bacillus subtilis* 168
RphC	RphB (80%)	*Paenibacillus* sp. LC231
RphD	RphB (78%)	*Paenibacillus* sp. LC231
BbI	BcI (60%)	*Bacillus cereus*
MphJ	MphI (51%)	*Paenibacillus* sp. LC231
CatV	CatU (60%)	*Paenibacillus* sp. LC231
ClbB	ClbB (100%)	*Brevibacillus brevis* NBRC 100599

Supplementary Table 3: Pair-wise comparison of antibiotic resistance enzymes with their closest orthologs mobilized in Gram-positive pathogens.

Resistance Enzyme	Closest Relative (% ID)	Host
ANT(4')-Ic	ANT(4’)-Ib (49%)	*Staphylococcus aureus*
AAC(6')-35	AAC(6’)-Ie-APH(2’’)-Ia (45%)	*Staphylococcus aureus*
ANT(6)-Ic	Aad(6)	*Enterococcus faecium*
RphC	n/a	
RphD	n/a	
BbI	BlaZ (38%)	*Staphylococcus aureus*
MphJ	MphC (41%)	*Staphylococcus aureus*
CatV	CatQ (57%)	*Clostridium perfringens*
ClbB	CfrC (60%)	*Clostridium botulinum*

Supplementary Table 4: Pair-wise comparison of antibiotic resistance enzymes with their closest orthologs mobilized in Gram-negative pathogens.

Resistance Enzyme	Closest Relative (% ID)	Host
ANT(4')-Ic	ANT(3")-IIb (38%)	*Acinetobacter* spp.
AAC(6')-35	AAC(6')-Ip (41%)	*Escherichia coli*
ANT(6)-Ic	ANT(6)-Ib (55%)	*Campylobacter fetus* subsp. *fetus*
RphC	n/a	
RphD	n/a	
BbI	CTX-M-121 (48%)	*Escherichia coli*
MphJ	MphB (42%)	*Escherichia coli*
CatV	Cat (48%)	*Campylobacter coli*
ClbB	n/a	

Supplementary Table 5: Kinetic constants of resistance enzymes identified in this study.

Enzyme	Substrate	K_m (μM)	k_{cat} (s^{-1})	K_i (μM)[a]	k_{cat}/K_m ($s^{-1}M^{-1}$)
ANT(4')-Ic	Kanamycin	0.56 ± 0.08	0.020 ± 0.001		3.5×10^4
	ATP	637 ± 66	0.022 ± 0.001		3.5×10^1
AAC(6')-35	Kanamycin	12 ± 8	-	12 ± 9	-
	Acetyl-CoA[b]	690 ± 90	0.18 ± 0.01		2.6×10^2
RphC	Rifampin	1.7 ± 0.6	0.091 ± 0.016	16 ± 7	4.9×10^4
	ATP	19 ± 2	0.057 ± 0.002		3.0×10^3
RphD	Rifampin	1.3 ± 0.4	0.13 ± 0.02	23 ± 11	1.0×10^5
	ATP	24 ± 3	0.089 ± 0.003		3.9×10^3
MphJ	Erythromycin	8.5 ± 1.2	0.37 ± 0.01		4.3×10^4
	Clarithromycin	17 ± 3	0.34 ± 0.02		2.0×10^4
	Telithromycin	16 ± 1	0.68 ± 0.01		4.2×10^4
	Azithromycin	3.7 ± 0.7	0.23 ± 0.01		6.1×10^4
	Tylosin	110 ± 30	0.56 ± 0.06		5.0×10^3
	ATP	1800 ± 860	0.04 ± 0.01		2.2×10^1
	GTP	20 ± 3	0.39 ± 0.02		1.9×10^4

a - K_i reflects substrate inhibition

b - The highest concentration of Acetyl-CoA used for K_m determination was 2000 μM, and therefore was not at saturation.

Supplementary Table 6: Oligonucleotides used for resistance gene cloning.

Gene	Vector	Primer Direction	Restriction Site	Sequence
catV	pET28a	Forward	*Nde* I	GGGCCCGCCATATGAAATTTCAGCGAATCGATCTAG
		Reverse	*Hind* III	AAGGGGCCAAGCTTTCACTCGACACCTAACCATTCC
mphJ	pET28a	Forward	*Nde* I	GGGCCCGCATATGTCAAAAAACAATGTAGAGCAC
		Reverse	*Hind* III	GGCGGGAAAAGCTTCTAGGAAGTGATCTCTTTGCC
ant(6)-Ic	pGDP4	Forward	*Nde* I	AAACCCCATATGGTGGCTTTGAGAACGG
		Reverse	*Xho* I	AAAGGGCTCGAGTCATTTCCACGAATGGTAG
ant(4')-Ic	pGDP4 (MIC experiments) pET28a (Overexpression and purification)	Forward	*Nde* I	AAAGGGAACATATGAACATGAATGGACCTG
		Reverse	*Xho* I	CCCACCCTCGAGTTAAAAAGGAATTCGCTCTG
aac(6')-35	pGDP4 (MIC experiments) pET28a (Overexpression and purification)	Forward	*Nde* I	TGTTTACATATGATTTATGCTGGTGATCTTACC
		Reverse	*Xho* I	AAATTTCTCGAGTTAATCAGCAGGAGCAATCCATTC
clbB	pGDP4	Forward	*Nde* I	AAACGCCATATGAAACTAACCTCGAAATATGAAAC
		Reverse	*Xho* I	CGAAATCTCGAGTTATTCAGAACGGTATAGCTGGC
bbI	pGDP4	Forward	*Bam* HI	ATCCTGGGATCCATGAAAGTTTACACATCGAGAC
		Reverse	*Xho* I	TTGGTCTCGAGTTACGGTTTTGCAGCCGTC

Supplementary Table 7: Oligonucleotides used for qPCR.

Gene	Organism	Direction	Sequence
mphJ	*B. brevis* VM4	Forward	ACGGAATCCTGGTAGACCCC
		Reverse	CCAATCCGGTACTTCGACACG
ant(4')-Ic	*B. brevis* VM4	Forward	CCTGCCAAGAAATTGCTGCG
		Reverse	CACATTCACTTCCGCCTTCC
aac(6')-35	*B. brevis* VM4	Forward	AGATGACGGTGAAACCCGC
		Reverse	GGAGGATGGCTGTAACGAGC
gyrA	*B. brevis* VM4	Forward	TATCGTCAGTCGGGCTTTGC
		Reverse	CTTGGGCCATACGTACCATCG
rphC and *rphD* (degenerate)	*B. brevis* VM4	Forward	ATTTTACAACTGGMACGCATYGG
		Reverse	ATCKCCMCGCTCYATGATGG
gyrA	*Paenibacillus* sp. LC231	Forward	CCGCTTCAGGCTCATCGC
		Reverse	ACCGGTTGTGGCACTTAAGG
mphI	*Paenibacillus* sp. LC231	Forward	CCGGAGCTCATCGCCTATCC
		Reverse	ACCTCTTGGGGACTCTTTACCC

References

Chang JM, Di Tommaso P, Notredame C. (2014). TCS: a new multiple sequence alignment reliability measure to estimate alignment accuracy and improve phylogenetic tree reconstruction. *Mol Biol Evol* **31**: 1625-1637.

Clinical and Laboratory Standards Institute 2012. Methods for dilution: antimicrobial susceptibility testing of bacteria that grow aerobically. Wayne, PA, USA: CLSI.

Cox G, Sieron A, King AM, De Pascale G, Pawlowski AC, Koteva K, et al. (2017). A Common Platform for Antibiotic Dereplication and Adjuvant Discovery. *Cell Chem Biol* **24**: 98-109.

Cox G, Stogios PJ, Savchenko A, Wright GD. (2015). Structural and molecular basis for resistance to aminoglycoside antibiotics by the adenylyltransferase ANT(2'')-Ia. *MBio* **6**.

Forsberg KJ, Patel S, Gibson MK, Lauber CL, Knight R, Fierer N, et al. (2014). Bacterial phylogeny structures soil resistomes across habitats. *Nature* **509**: 612-6.

Hu Y, Yang X, Li J, Lv N, Liu F, Wu J, et al. (2016). The Bacterial Mobile Resistome Transfer Network Connecting the Animal and Human Microbiomes. *Appl Environ Microbiol* **82**: 6672-6681.

Jia B, Raphenya AR, Alcock B, Waglechner N, Guo P, Tsang KK, et al. (2017). CARD 2017: expansion and model-centric curation of the comprehensive antibiotic resistance database. *Nucleic Acids Res* **45**: D566-d573.

Katoh K, Standley DM. (2013). MAFFT multiple sequence alignment software version 7: improvements in performance and usability. *Mol Biol Evol* **30**: 772-780.

Kessler N, Schuhmann H, Morneweg S, Linne U, Marahiel MA. (2004). The linear pentadecapeptide gramicidin is assembled by four multimodular nonribosomal peptide synthetases that comprise 16 modules with 56 catalytic domains. *J Biol Chem* **279**: 7413-9.

Lee JY, Janes BK, Passalacqua KD, Pfleger BF, Bergman NH, Liu H, et al. (2007). Biosynthetic analysis of the petrobactin siderophore pathway from *Bacillus anthracis*. *J Bacteriol* **189**: 1698-710.

Li LG, Xia Y, Zhang T. (2017). Co-occurrence of antibiotic and metal resistance genes revealed in complete genome collection. *ISME J* **11**: 651-662.

Maglott D, Ostell J, Pruitt KD, Tatusova T. (2007). Entrez Gene: gene-centered information at NCBI. *Nucleic Acids Res* **35**: D26-31.

Mootz HD, Marahiel MA. (1997). The tyrocidine biosynthesis operon of *Bacillus brevis*: complete nucleotide sequence and biochemical characterization of functional internal adenylation domains. *J Bacteriol* **179**: 6843-50.

Pawlowski AC, Wang W, Koteva K, Barton HA, Mcarthur AG, Wright GD. (2016). A diverse intrinsic antibiotic resistome from a cave bacterium. *Nat Commun* **7**: 13803.

Shakya T, Wright GD. (2010). Nucleotide selectivity of antibiotic kinases. *Antimicrob Agents Chemother* **54**: 1909-1913.

Sievers F, Wilm A, Dineen D, Gibson TJ, Karplus K, Li W, et al. (2011). Fast, scalable generation of high-quality protein multiple sequence alignments using Clustal Omega. *Mol Syst Biol* **7**: 539.

Smillie C, Garcillan-Barcia MP, Francia MV, Rocha EP, De La Cruz F. (2010). Mobility of plasmids. *Microbiol Mol Biol Rev* **74**: 434-52.

Spanogiannopoulos P, Waglechner N, Koteva K, Wright GD. (2014). A rifamycin inactivating phosphotransferase family shared by environmental and pathogenic bacteria. *Proc Natl Acad Sci U S A* **111**: 7102-7.

Stamatakis A. (2014). RAxML version 8: a tool for phylogenetic analysis and post-analysis of large phylogenies. *Bioinformatics* **30**: 1312-1313.

Stogios PJ, Cox G, Spanogiannopoulos P, Pillon MC, Waglechner N, Skarina T, et al. (2016). Rifampin phosphotransferase is an unusual antibiotic resistance kinase. *Nat Commun* **7**: 11343.

Theodore CM, Stamps BW, King JB, Price LS, Powell DR, Stevenson BS, et al. (2014). Genomic and metabolomic insights into the natural product biosynthetic diversity of a feral-hog-associated *Brevibacillus laterosporus* strain. *PLoS One* **9**: e90124.

Weber T, Blin K, Duddela S, Krug D, Kim HU, Bruccoleri R, et al. (2015). antiSMASH 3.0-a comprehensive resource for the genome mining of biosynthetic gene clusters. *Nucleic Acids Res* **43**: W237-43.

Westman EL, Yan M, Waglechner N, Koteva K, Wright GD. (2013). Self resistance to the atypical cationic antimicrobial peptide edeine of *Brevibacillus brevis* Vm4 by the N-acetyltransferase EdeQ. *Chem Biol* **20**: 983-90.

Wright GD, Ladak P. (1997). Overexpression and characterization of the chromosomal aminoglycoside 6'-N-acetyltransferase from Enterococcus faecium. *Antimicrob Agents Chemother* **41**: 956-60.